

An experimental study of the spectrum of spin waves localized on a Bloch line

L. M. Dedukh, Yu. P. Kabanov, and V. I. Nikitenko

Institute of Solid State Physics, Academy of Sciences of the USSR

(Submitted 17 July 1989)

Zh. Eksp. Teor. Fiz. **97**, 570–577 (February 1990)

The dependence of the amplitude of forced oscillations of Bloch lines in an yttrium iron garnet on the frequency of the exciting field is investigated using a magneto-optic method. Local photometry and direct observation of the oscillating Bloch line permits the study of the characteristics of specific standing spin waves that occur at definite frequencies in the bending oscillations of the Bloch line. For the first time, the dispersion law of the oscillations is determined. It is shown that Bloch points are present at the nodes of the elliptically polarized standing waves that are being investigated. These arise near the wafer surface and have a significant influence on the characteristics of the bending of the whole Bloch line.

INTRODUCTION

As is well known, it has long since been rigorously proved¹ that in the basic thermodynamic equilibrium state of a real noninfinite crystal the distribution of the magnetization is spatially inhomogeneous. The minimum value of the total free energy, taking account of the demagnetizing field due to the presence of a magnetization component normal to the body surface, is achieved in the majority of cases when there are stable ordered state defects formed in the sample—Bloch walls, lines, and even points.²

This fact has, however, still not received sufficient attention in the analysis of the excited state of an iron garnet. At present, the spectrum of spin waves in a homogeneously magnetized crystal has been well studied,³ and we already have a number of theoretical and experimental papers^{2,4–14} devoted to studying the magnon spectrum in a uniform domain boundary. But the study of the spectrum of the spin waves that are localized on a Bloch line has practically still to begin.

Meanwhile, analysis of this problem is of fundamental interest for solving both fundamental and practical problems. It has been convincingly demonstrated in recent years that Bloch lines are characterized by singularities that are characteristic of vortex-like solitons.^{15–17} They are not only essential elements of the structure of a strongly excited state of the domain boundary (and often of its ground state as well), but also determine its dynamical properties to a significant extent. Without knowing the spectrum of the magnons localized on the Bloch line, it is impossible to develop a general theory of the elementary and nonlinear excitations in ferromagnetism, or to construct a microscopic theory of the processes for magnetizing it which are due to displacement of the domain boundaries, or to carry out rigorous calculations concerning the operational reliability of new ultrahigh-capacity computer magnetic memory elements that use Bloch lines as information carriers.

In this paper, we give the first experimental data concerning the spectrum of magnons localized on a Bloch line, these data being obtained using a method we have previously described.¹⁸ They are compared with the only theoretical treatment completed recently.¹⁹

EXPERIMENTAL METHODOLOGY

The investigations were carried out on a single crystal wafer of yttrium iron garnet with dimensions

$\approx 0.8 \times 0.35 \times 0.025$ mm. It contained five 180-degree-domain boundaries, which divided bands magnetized along the $\langle 111 \rangle$ directions, parallel to the long edge and the (112) surface of the sample. In each boundary there was, as a rule, only one Bloch line in all (depending on the remagnetization conditions). Specific closed domains were observed on the ends of the wafer.²⁰ The magnetic field associated with the magnetization vectors in a wall emerging onto the wafer surface caused the Bloch line to distort and deviate from the normal to the wafer (Fig. 1).

In a transmission polarizing microscope with crossed Nicol prisms, this Bloch line was visible on the xy representation plane as a dark band between the bright subdomains in the wall that appeared as a result of Faraday effects of opposite sign in them (Fig. 2a). This enabled us to carry out direct observation of the change in the form of a line under the influence of external forces. Using a rectangular diaphragm, whose dimensions were regulated micrometrically, it was possible to distinguish different parts of the black and white representation of the domain wall with the Bloch line that was directed into a photomultiplier for photometry, and thus study the oscillation characteristics of these parts. To measure the oscillations of the Bloch line along the wall (parallel to the x axis), the microscope Nicol prisms were slightly uncrossed so that neighboring subdomains were colored black and white on account of the Faraday effect (shown schematically in Fig. 3). The motion (along the y axis) of the Bloch line together with the boundary was studied using the displacement of the portion of the wall adjacent to it with crossed Nicol prisms and in a situation where the rectangular diaphragm was confined to half of the representation of the domain wall and part of the neighboring domain. In this case, we used black–white contrast on the boundary between the domain and the wall itself.

The signal from the photomultiplier was recorded on the SK4-59 spectrum analyzer. For phase analysis of the magneto-optic signal, we used a MODEL 5202 selective amplifier. The magnetic fields were created using Helmholtz coils of radius 6 mm.

EXPERIMENTAL RESULTS

The curves 1–3 in Fig. 3 show the frequency dependence of the intensity J of the magneto-optic signal, which is proportional to the amplitudes of oscillation of different parts of the Bloch line along the domain wall, the frequency

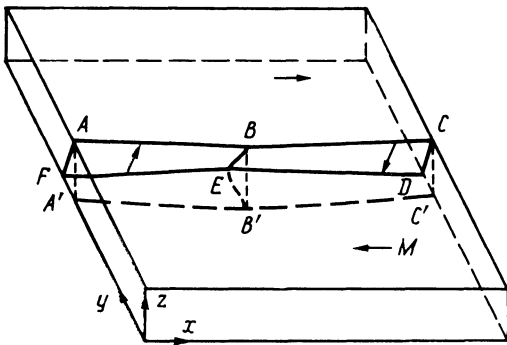


FIG. 1. Schematic diagram of the position of a domain boundary (ACDF) with a Bloch line (BE) in the sample and the magnetization distribution in it. FDC'A' and EB' are projections of the wall and the line, respectively, onto their representation plane in a polarizing microscope.

ν of the external magnetic field H_z that acts perpendicular to the sample surface, and the magnetization \mathbf{M} in the domains. Curve 1 was recorded with photometry of the whole Bloch line, curve 2 was recorded with photometry of its lower half, and curve 3 was recorded with photometry of its upper half (see the schemes in Fig. 3). It can be seen that traces 2 and 3 are different from 1 and have sharply marked peaks at the same frequencies. Photographs of a Bloch line performing forced oscillations at the resonance frequencies ν_n corresponding to these peaks are shown in Fig. 2b-d. The erosion of the line representation in these photographs is due to oscillation of the whole line or separate parts of it to great distances along the wall. The black dots that appear in the Bloch line representation at $\nu = 0.95$ MHz and $\nu = 1.8$ MHz (Fig. 2b, c), signify that their corresponding parts of the wall do not oscillate at these frequencies. As phase analysis demonstrates, the sections of the Bloch line that are separated by these points oscillate along the x axis with a phase shift that differs from π by several degrees.

At frequencies corresponding to the peaks described above, we also recorded displacement resonances of the Bloch line (or of parts of it) along the y axis. Measuring the phase of the oscillations of the upper and lower halves of the domain wall near the line at the frequencies of the first two resonance peaks demonstrated that they oscillate with a phase shift of several degrees.

All these data give evidence that, under the conditions of the experiment presented here, there appeared specific standing spin waves localized on the Bloch line. According to the photographs of Fig. 2b-d, at a frequency $\nu_0 = 0.4$

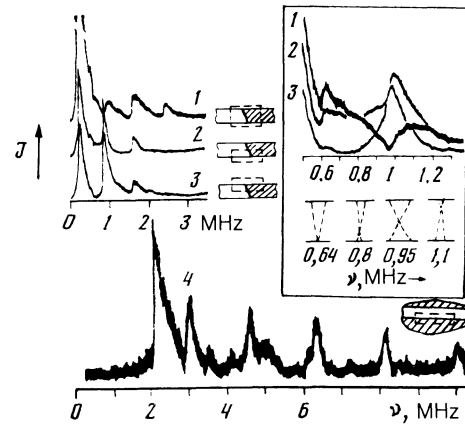


FIG. 3. Magneto-optic signal J , proportional to the displacement of the Bloch line along the wall (curves 1-3) vs the frequency ν of the magnetic field H_z , measured by photometry of the whole line (1), and its upper (2) and lower (3) halves. $H_z^0 = 225$ mOe. Curve 4 is the magneto-optic signal, reflecting the amplitude of the oscillation of a monopolar domain boundary, as a function of the H_x field frequency (with amplitude $H_x^0 = 15$ mOe), parallel to the magnetization in the domains. It was obtained from photometry of half of the width of the representation of the oscillating boundary in an additional constant field $H_z = 24$ Oe, which stabilizes the state of the boundary. The parts undergoing photometry are bounded by a rectangle on the schematic diagrams given near each curve. The diagrams in the insert characterize the amplitudes of the oscillations of various parts of the Bloch line.

MHz the first peak of the $J(\nu)$ dependence produces homogeneous resonance oscillations of the Bloch line. At $\nu_1 = 0.95$ MHz, one half of the standing wave ($n = 1$), whose node is located at the middle of the Bloch line, lies along the oscillating line. The third peak in the $J(\nu)$ dependence corresponds to $n = 2$ ($\nu_2 = 1.8$ MHz). Figure 4 gives a schematic representation of the trajectories of the motion of the Bloch line, where this motion forms a standing wave with one node, and the trajectories are constructed assuming that the Bloch line oscillations are elliptically polarized. The long axes of the strongly extended trajectories of opposing parts of the line are slightly inclined to the x axis on different sides.

Curve 4 in Fig. 3 shows the frequency dependence of the intensity of the magneto-optic signal due to the forced oscillations of this same domain wall in a monopolar state. It is measured in the constant wall-magnetizing field H_z according to the method described in Ref. 14. The sharply pronounced peak on it are connected with the excitation of standing kink waves of the whole wall around an axis paral-

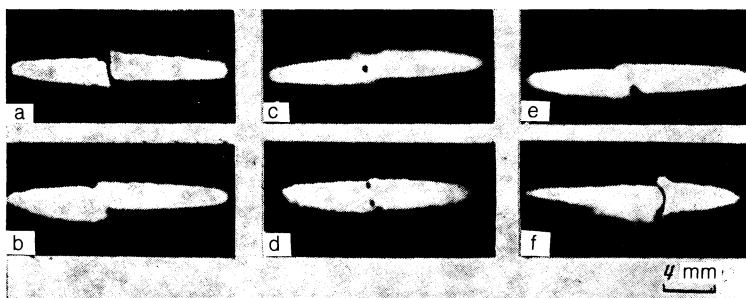


FIG. 2. Representation in an optical polarizing microscope of part of a domain wall with one Bloch line at $H_z^0 = 0$ (a, f) and $H_z^0 = 225$ mOe, $\nu = 0.4$ MHz (b), 0.95 MHz (c), 1.8 MHz (d), 0.64 MHz (e); $f-H_y = 7.75$ Oe. The Nicol prisms are crossed. The length of the representation of the wall is determined by the diameter of the laser beam in the focal plane.

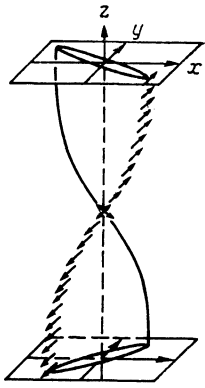


FIG. 4. Trajectories of Bloch line motion (shown on the xy plane) at neighboring crests of a standing wave and spin polarization (arrows) in the core of the Bloch line. A Bloch point is located at the node of the wave.

nel to the magnetization direction in the neighboring domains.¹⁴ Measurements have demonstrated that the upper and lower halves of the wall oscillate practically in antiphase at the frequency corresponding to the first peak in curve 4, and in phase at the frequency of the second peak of this curve. This bears witness to the fact that the first peak is determined by kink oscillations of the wall with $n = 1$, and the second peak corresponds to $n = 2$. We may assume that the following peaks in curve 4 also reflect the excitation of the following even and odd modes of the kink oscillations of the wall (when it is not attached to the sample surface). As can be seen from comparing the curves in Fig. 3, the resonance frequencies that correspond to pure oscillation modes of the Bloch line and of the monopolar wall are clearly distinguished from each other.

The standing waves on the Bloch lines manifested themselves as resonance peaks in the $J(\nu)$ dependences when the diaphragm was positioned so that complete compensation of the Faraday effect due to partial screening of neighboring subdomains along the light beam upon oscillation of the Bloch line is not achieved. Therefore, as a rule, the standing waves did not all appear on the line at one position of the diaphragm confining the photometric light. In particular, in curve 1 of Fig. 3, which was obtained from photometry of the whole Bloch line, we observe the minimum value of J at the frequency corresponding to $n = 1$. At the same time, in this curve there appeared a peak corresponding to a wave with $n = 3$ ($\nu_3 = 2.5$ MHz).

The insert in Fig. 3 gives curves 1–3 in a close-up view for a small frequency range and, in contrast to the curves in the main figure, they are not dispersed along the ordinate axis. Beneath them is a schematic representation of the amplitudes with which various parts of the Bloch line deviate from the equilibrium position, determined from direct observation of the line and phase analysis of the magneto-optic signal at various frequencies. In all the curves, another small peak is clearly visible at $\nu_n = 0.64$ MHz. The representation of the line in polarized light at this frequency shown in Fig. 2d (see also the inset diagram at $\nu = 0.64$ MHz) gives evidence that one end of the line is fixed under these conditions. Therefore, the peak in the $J(\nu)$ dependence at $\nu_n = 0.64$ MHz may be determined by the quarter-wave resonance of the Bloch line, for which $n = 1/2$.

As the frequency H_z of the field increased, the node that had formed moved into the interior of the crystal. It divided the line into parts that were oscillating almost in antiphase.

Therefore, the total signal (curve 1 given by photometry of the whole Bloch line) fell to its minimum value, with the node located in the middle of the Bloch line, although the oscillation amplitude of its opposite parts reached the maximum value (see curves 2 and 3 and the schematic diagram at $\nu = 0.95$ MHz). As ν increased further, the nonoscillatory part of the oscillating line continued to change its position. A second node of the wave with $n = 2$ appeared near the same surface of the wafer where the first one was formed. As ν decreased, the nonoscillatory part of the line moved in the opposite direction.

Under the influence of an additional constant magnetic field H_y , perpendicular to the domain wall, the node of a standing wave on the Bloch line (with $\nu = \text{const}$) moved along the domain wall in one direction or the other, depending on the polarity of H_y in the same way as a Bloch point on a Bloch line oscillating under the influence of gyrotropic forces.²¹ When this nonoscillatory part had passed along the whole line (in the H_y field), the phase of its homogeneous oscillations along the wall excited by a magnetic field H_x , parallel to the magnetization in the domains, changed by an amount $\approx \pi$.

Under the influence of the field H_y , “magnetization” (or “remagnetization”) of the Bloch line occurred. Therefore, the result we have described gives evidence that a Bloch point is located in the node of a standing wave on the line, which divides it into quasidomains with an opposite spin polarization along the y axis (Fig. 4). In a constant field H_y (some oersteds in magnitude) the appearance of a Bloch point in the process of recording the $J(\nu)$ curves occurred near the upper or lower surface of the wafer, depending on the polarity of the H_y field.

Figure 5 shows the position of the Bloch point on a line oscillating in a field as a function H_x , of the field H_y magnetizing the wall. Each value of H_y corresponding to a position z was obtained from a large number of measurements. The sizable scatter in the experimental results prevents us from distinguishing hysteresis phenomena. This dependence indicates that, practically speaking, in the absence of an external field H_y the Bloch line is magnetized in a single direction. Therefore, when a standing wave forms as the frequency is varied, the Bloch point “enters” from the same end of the Bloch line. Signs of a change in the structure of the Bloch line in the H_y field are also observed in its static representation in the absence of a variable field (Fig. 2e).

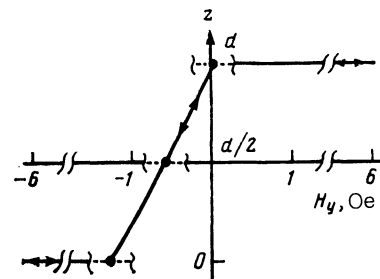


FIG. 5. Position of the Bloch point in a Bloch line oscillating in a field H_x ($H_x^0 = 90$ mOe, $\nu = 0.5$ MHz), as a function of the magnetic field strength H_y .

DISCUSSION

Figure 6 displays the dependence of the resonance frequency ν_n of a peak on its order $n = 2d/\lambda = (d/\pi)k$ (where d is the line length, and λ and k are the wavelength and wave vector respectively) for an oscillating Bloch line (Fig. 1). Here is shown also the analogous dependence for kink oscillations of a monopolar wall (curve 2) constructed using curve 4 from Fig. 3. They characterize the dispersion laws of the kink waves of a Bloch line and domain boundary whose wave vectors are perpendicular to the wafer surface. It can be seen that the dispersion curve for the Bloch line is lower than the curve for the wall. Note that the character of the experimentally obtained dispersion dependence of the domain boundary bending oscillations corresponds qualitatively to that calculated in Ref. 2 for waves propagating perpendicular to an axis of easy magnetization in the presence of an external gradient field that stabilizes the domain wall.

The size of the gap in the Bloch line oscillation spectrum is determined by the frequency of the translational resonant oscillations of the line ($\omega_0 = 2\pi\nu_{n=0}$) and is equal to ≈ 2.5 MHz. From the width $\Delta\nu_{n=0}$ of the resonance peak, we can estimate both the dissipation parameter α in the Landau-Lifshits equation for the motion of the magnetic moment, and also the viscosity coefficient β_x in the equation of motion of the Bloch line²:

$$\alpha = \Delta\nu_{n=0}/2M\gamma \approx 0.5 \cdot 10^{-4},$$

$$\beta_x = \Delta\nu_0 \kappa_x / 2\pi\nu_n^2 \approx 1.3 \cdot 10^{-6} \text{ g/cm s.}$$

Here γ is the gyromagnetic ratio. The coefficient κ_x characterizes the elastic force that restores the Bloch line towards its original position as it moves along the x axis. Its magnitude (40 erg/cm^3), as well as the value $\kappa_y = 4.6 \times 10^{-4} \text{ erg/cm}^2$ of the analogous coefficient that characterizes the elastic force acting on the line as it moves along the y axis, were determined from measuring the dependence of the line displacement along the wall along with the strength of the static fields H_z and H_x respectively.^{15,16}

Curve 3 in Fig. 6 was calculated on the basis of the formula

$$\omega_n^2 = \omega_0^2 \left\{ 1 + \left[\left(\frac{\sigma_x}{\kappa_x} + \frac{\sigma_y}{\kappa_y} \right) \left(\frac{\pi}{d} n \right)^2 + \frac{\sigma_x \sigma_y}{\kappa_x \kappa_y} \left(\frac{\pi}{d} n \right)^4 \right] \right\}, \quad (1)$$

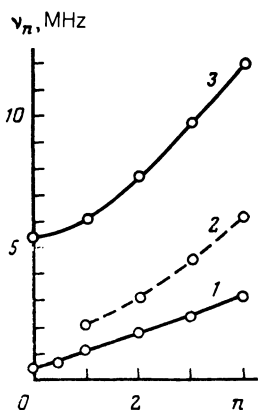


FIG. 6. Dependence of ν_n , the resonance frequency of a peak, on its order n , determined from the data of Fig. 3 for a Bloch line (curve 1) and a monopolar wall (curve 2). Curve (3) is calculated according to (1).

where $\omega_0^2 = (\gamma/2\pi M)^2 \kappa_x \kappa_y$, and $\omega_n = 2\pi\nu_n$, that was obtained in Ref. 19 and describes the bending oscillation spectrum of a monopolar Bloch line. In calculating this curve, we assumed that the Bloch line strain components were $\sigma_y = \sigma_x = 8AQ^{-1/2}$. From comparing curve 1 with curve 3, it can be seen that the experimentally determined spectrum of the spin waves localized on the Bloch line differs from that constructed theoretically both in the character of the dependence of σ_n on n (that is, of ω on k) and in the size of the gap. Taking account of the demagnetizing field that appears when κ_x is measured does not remove these differences.

The basic cause of the differences that manifest themselves apparently lies in the fact that the theoretical model¹⁹ does not take account of the field of the magnetostatic charges that are associated with the crystal surface and are due to an inhomogeneous magnetization distribution along the Bloch line, and which also exist on it in the static state and appear due to kink oscillations. The inhomogeneity of the spin distribution along the Bloch line manifests itself in experiments to measure the effect of a constant field H_y on the position of the Bloch point on it (see Fig. 5). The experimentally observed alteration in the structure of the Bloch line (formation and movement of Bloch points) as the frequency of the stimulated oscillations changes may also be explained quantitatively by taking account of the inhomogeneity of the spin distribution along the line. It should be emphasized that the standing waves on a Bloch line (with $n \leq 4$) that have been observed in the experimental situations described above always contained Bloch points at the nodes.

In Ref. 19 an expression was also obtained for the frequency of the characteristic oscillations of a Bloch line at whose center there is a Bloch point that is oscillating with significantly smaller amplitudes than is the line. It has the form of (1) for $n = 1$, without the last term on the right hand side. The value of $\omega_1/2\pi$ calculated from this is practically coincident with the second point on curve 3 of Fig. 6. According to Ref. 19 the differences in the experimentally measured and calculated magnitudes of the gap and the oscillation eigenfrequencies of a line with a Bloch point cannot be explained by the influence of the aftereffect.¹⁴ They may arise because the coefficients κ_x and κ_y differ from those determined experimentally in quasistatic conditions when the line is displaced to distances greater than the amplitude of its induced oscillations. Taking account of this fact leads to still greater contradictions with the experimental data. We note, finally, that the inhomogeneity of the spin distribution along the Bloch line, as well as errors in determining κ_x and κ_y , which may be due to a difference between the theoretical and experimental values of ω_0 , may also be determined by the peculiarities of the domain structure of a sample that contains specific closed domains and several walls with single Bloch lines.

CONCLUSION

Thus, as a result of the experiment we have carried out, we have succeeded in determining for the first time the basic characteristics of the long-wavelength portion of the spectrum of the spin waves localized on a Bloch line. We have observed that the standing wave nodes contain Bloch points. Their nucleation and motion along the Bloch line has an effect on the characteristics of the kink oscillations of the wall. We give data confirming that in order to describe the

dispersion law that was determined in the experiment it is necessary to take account of the inhomogeneity in the spin distribution along the Bloch line and the change in this distribution under the influence of external magnetic fields.

- ¹L. D. Landau and E. M. Lifshitz, *Phys. Z. Sowjetunion* **8**, 135 (1935).
²A. P. Malozemoff and J. C. Slonczewski, *Magnetic domain walls in bubble materials* (Academic, New York–London–Toronto–Sydney–San Francisco, 1979) (Russ. Trans. Mir, Moscow, 1982).
³A. I. Akhiezer, V. G. Bar'yakhtar, and S. V. Peletminskiĭ, *Spinovye volny* (Spin waves) (Mir, Moscow, 1982); Engl. Trans. North Holland, Amsterdam (1968).
⁴J. F. Winter, *Phys. Rev.* **124**, 452 (1961).
⁵J. F. Janak, *Phys. Rev.* **134**, A411 (1964).
⁶M. M. Farztdinov and E. A. Turov, *Fiz. Metall. Metalloved.* **29**, 458 (1970).
⁷M. I. Kurkin and A. P. Taneev, *Fiz. Metall. Metalloved.* **36**, 1149 (1973).
⁸A. A. Thiele, *Phys. Rev. B* **7**, 391 (1973).
⁹E. Schlömann, *IEEE Trans. Magn.* **10**, 11 (1974).
¹⁰I. A. Glinskiĭ, *Zh. Eksp. Teor. Fiz.* **68**, 1032 (1975) [*JETP* **41**, 511 (1975)].

- ¹¹A. E. Borovik, V. S. Kuleshov, and M. A. Strzhemechniy, *Zh. Eksp. Teor. Fiz.* **68**, 2236 (1975) [*JETP* **41**, 1118 (1975)].
¹²J. C. Slonczewski, *J. Appl. Phys.* **55**, (IIB), 2536 (1984).
¹³B. E. Argyle, J. C. Slonczewski, W. Jantz *et al.*, *IEEE Trans. Magn.* **18**, 1325 (1982).
¹⁴L. M. Dedukh, V. I. Nikitenko, and V. T. Synogach, *Zh. Eksp. Teor. Fiz.* **94**, 312 (1988) [*Sov. Phys. JETP* **67**, 1912 (1989)].
¹⁵V. S. Gornakov, L. M. Dedukh, Yu. P. Kabanov, and V. I. Nikitenko, *Zh. Eksp. Teor. Fiz.* **82**, 2007 (1982) [*JETP* **55**, 1154 (1982)].
¹⁶V. S. Gornakov, L. M. Dedukh, and V. I. Nikitenko, *Zh. Eksp. Teor. Fiz.* **94**, 245 (1988) [*JETP* **67**, 570 (1984)].
¹⁷A. V. Nikiforov and E. B. Sonin, *Pis'ma Zh. Eksp. Teor. Fiz.* **40**, 325 (1984) [*JETP Lett.* **40**, 1119 (1984)].
¹⁸Yu. P. Kabanov, L. M. Dedukh, and V. I. Nikitenko, *Pis'ma Zh. Eksp. Teor. Fiz.* **47**, 638 (1988) [*JETP Lett.* **47**, 737 (1988)].
¹⁹Yu. A. Kufaev and E. B. Sonin, *Fiz. Tverd. Tela* **30**, 3272 (1988) [*Sov. Phys. Solid State* **30**, 1882 (1988)].
²⁰V. K. Vlasko-Vlasov, L. M. Dedukh, and V. I. Nikitenko, *Zh. Eksp. Teor. Fiz.* **71**, 2291 (1976) [*JETP* **44**, 1208 (1976)].
²¹Yu. P. Kabanov, L. M. Dedukh, and V. I. Nikitenko, *Pis'ma Zh. Eksp. Teor. Fiz.* **49**, 551 (1989) [*JETP Lett.* **49**, 637 (1989)].

Translated by Howard Turner